University of Brasília
Institute of Exact Sciences
Department of Statistics

Master's Dissertation

A new invertible bimodal Weibull model

by

Beatriz Leal Simões e Silva

Brasília, November 2022

A new invertible bimodal Weibull model

by

Beatriz Leal Simões e Silva

A dissertation submitted to the Departament of Statistics at the University of Brasília in partial fulfilment of the requirements for the degree Master in Statistics.

Supervisor: Prof. Dr. Cira Etheowalda Guevara Otiniano
Co-supervisor: Prof. Dr. Eduardo Yoshio Nakano

Brasília, November 2022

A dissertation submitted to the Departament of Statistics at the University of Brasília in partial fulfilment of the requirements for the degree Master in Statistics.

Approved by:

Prof. Dr. Cira Etheowalda Guevara Otiniano

Supervisor, EST/UnB

Prof. Dr. Eduardo Yoshio Nakano

Cosupervisor, EST/UnB

Prof. Dr. Helton Saulo Bezerra dos Santos

EST/UnB

Prof. Dr. Marcelo Bourguignon Pereira

EST/UFRN

All models are wrong, but some are useful.

(George Box)

To my family and friends.

Acknowledgments

Resumo Expandido

UM NOVO MODELO WEIBULL BIMODAL INVERSÍVEL

A distribuição Weibull introduzida por Waloddi Weibull em 1951, é um dos modelos mais utilizados em probabilidade e estatística, pois possui uma expressão simples para a função de densidade de probabilidade (FDP), função de densidade acumulada (FDA), função de sobrevivência e momentos. No entanto, a distribuição Weibull não é capaz de ajustar dados bimodais. O livro de Rinne (2009) fornece uma descrição detalhada da distribuição Weibull de três parâmetros, desde sua introdução até suas aplicações. Nas últimas duas décadas, muitas generalizações e extensões da distribuição Weibull foram propostas a fim de fornecer maior assimetria e bimodalidade na FDP, bem como flexibilizar a função de risco (HRF) para formas não monotônicas, como banheira, unimodal, M ou N.

Para essas generalizações, algumas técnicas foram aplicadas a várias outras famílias de distribuições. Dentre essas técnicas, podemos citar a família de distribuição exponencial, família de distribuição beta, família de distribuição beta modificada, família de distribuição de potência generalizada. Algumas dessas distribuições são Weibull exponencializadas (Mudholkar and Srivastava, 1993), *beta-Weibull* (Lee, Famoye, and Olumolade, 2007), *modified Weibull* (Zaindin and Sarhan, 2009), *power generalized Weibull* (Kumar and Dey, 2017) , *Exponentiated Power Generalized Weibull* (Pena-Ramirez et al., 2018). Todos esses modelos apresentam 3 ou mais

parametros, são unimodais e possuem a distribuição Weibull como caso particular.

No contexto de populações heterogêneas com duas modas, as generalizações da distribuição Weibull são recentes na literatura. Saboor et al., (2019) propuseram a distribuição *modified beta modified-Weibull* com seis parâmetros. Uma desvantagem desse modelo é que sua FDA não possui uma forma fechada simples. Nota-se também que uma mistura de duas distribuições Weibull é um modelo natural para capturar a bimodalidade (McLachlan and Peel, 2000), entretanto, as propriedades e o procedimento para estimar seus parâmetros podem dificultar suas aplicações

Recentemente, Vila e Çankaya (2021) usaram uma técnica de transformação quadrática para gerar uma distribuição Weibull bimodal. Este modelo é uma mistura de três distribuições Weibull. A FDA é expressa em termos da função incompleta Gama. Ou seja, suas funções FDA e quantil não possuem formas fechadas, que seriam muito úteis para procedimentos como simulação e cálculos de medidas de risco.

Neste trabalho, propomos uma nova generalização da distribuição de Weibull. Dois modelos são apresentados, Weibull Bimodal Invertível (IBW) e seu caso particular, Weibull Bimodal Invertível Não Negativa (NNIBW). Em ambos os modelos, a FDP apresenta várias formas de assimetria. A FDA tem uma expressão fechada simples e invertível, então sua função quantil também possui uma fórmula fechada simples. Isso torna o modelo atrativo para ser usado em procedimentos de simulação, regressão e cálculo de medidas de risco em diversas áreas. Por exemplo, em finanças para o cálculo do *Value at Risk (VaR)*, em hidrologia para o cálculo do tempo de retorno (RT) e em confiabilidade para o cálculo da HRF. O HRF pode assumir formas monótonas, unimodais, banheira ou em forma de N.

Na seção 1.2, é apresentada os modelos IBW e NNIBW, assim como seus cálculos e definições importantes, suas funções densidade de probabilidade, além de materiais como momentos, função quantil, estatísticas de ordem, sobrevivência e funções de risco.

Na seção 1.3, é detalhada a função de máxima verossimilhança para o modelo NNIBW, que é utilizada para a estimação dos parâmetros do modelo, em seguida a performance do modelo é testada e detalhada via simulações Monte Carlo para 14 conjuntos de valores dos parâmetros

da distribuição. Utilizando o Erro Quadrático Médio (EQM), a distribuição apresentou bons resultados para a simulação.

Finalmente, na seção 1.4, o modelo é utilizado para analisar 4 conjuntos de dados reais referentes a temperatura ao longo de diferentes períodos. Para cada local, é feita uma transformação exponencial na variável da temperatura a fim de obter dados não negativos. Os modelos NNIBW e BWeibull (Vila and Niyazi Çankaya, 2021) são ajustados para cada conjunto de dados e graficamente nota-se um melhor ajuste bimodal da distribuição proposta. Também é detalhada a série temporal de cada localidade, suas funções acumuladas empíricas e teóricas, os quantis e por fim, as tabelas e gráficos de tempo de retorno das variáveis originais e ajustadas.

O modelo de regressão é ajustado para os dados da cidade de Yellowknife, utilizando as estações do ano como covaráveis. O modelo permite explicar a relação e influência da variável explicativa como evento de interesse, neste caso, as estações se mostraram tanto unimodais quanto bimodais, suas modas são explicadas pela variação de temperatura nas estações de transição primavera e o outono. Os resultados mostraram um desempenho satisfatório do modelo NNIBW para dados bimodais, sua função de forma fechada torna o modelo vantajoso para mais estudos em dados desta natureza em trabalhos futuros.

Palavras-Chave: Distribuição Weibull, Weibull Bimodal, Dados heterogêneos, Tempo de retorno

Abstract

The Weibull distribution is one of the most used models in statistics and applied areas, as it has a simple expression for the probability density function, survival function, and moments. However, the Weibull distribution is not able to fit bimodal data. In this work, we propose a new generalization of the three-parameter Weibull distribution, a new invertible bimodal Weibull model (NIBW), which can be bimodal and its cumulative distribution function and quantile function have a simple and closed form, which makes it very interesting in simulation procedures and for the calculation of risk measures in the applied areas. Several properties of the model were studied and the non-negative version of the model (NNIBW) was used in the performance of the maximum likelihood estimates of the parameters and tested using Monte Carlo simulation. Furthermore, using four sets of temperature data, we fitted and compared our model with another bimodal distribution, calculate the return time and fit as well a regression model for one chosen dataset.

Keywords: Weibull distribution, Bimodal Weibull, Heterogeneous data, Return time

Contents

Chapter 1

A new invertible bimodal Weibull model

1.1 Introduction

In probability and statistics, the Weibull distribution, introduced by Waloddi Weibull in 1951 is one of the most popular continuous probability models. It is widely used in many fields such as physics, biology, health, hydrology, and engineering, among others. Rinne's Book (2009) provides a detailed description of the three-parameter Weibull distribution, from its genesis to its applications. Its applicability in the reliability area is limited due to the monotonic form of its hazard rate function (HRF).

A continuous random variable Y has a Weibull distribution, $Y \sim F_{\beta,\mu,\lambda}$, if its probability density function (PDF) and cumulative distribution function (CDF) are given, respectively, by:

$$f_{\beta,\mu,\lambda}(y) = \begin{cases} \exp\left\{-\left[\frac{y-\mu}{\lambda}\right]^{\beta}\right\} \frac{\beta}{\lambda} \left[\frac{y-\mu}{\lambda}\right]^{\beta-1}, & y \geq \mu \\ 0, & y < \mu \end{cases} \tag{1.1.1}$$

and

$$
F_{\beta,\mu,\lambda}(y) = \begin{cases} 1 - \exp\left\{ - \left[\frac{y-\mu}{\lambda} \right]^{\beta} \right\}, & y \geq \mu \\ 0, & y < \mu, \end{cases} \tag{1.1.2}
$$

where $\beta > 0$ is shape parameter, $\lambda > 0$ scale parameter, and $\mu \in \mathbb{R}$ location parameter.

In the last two decades, many generalizations and extensions of the Weibull distribution have been proposed to provide greater asymmetry and bimodality in the PDF, as well as to flex the HRF for non-monotonic shapes such as bathtub, unimodal, M, or N shape.

For these generalizations, some techniques were already applied to several other families of distributions. Among these techniques, we can cite the exponentiated distribution family, beta distribution family, modified beta distribution family, generalized power distribution family. Some of these distributions are Weibull exponentialized (Mudholkar and Srivastava, 1993), beta-Weibull (Lee, Famoye, and Olumolade, 2007), modified Weibull (Zaindin and Sarhan, 2009), power generalized Weibull (Kumar and Dey, 2017) , Exponentiated Power Generalized Weibull (Pena-Ramirez et al., 2018). All these models have unimodal PDF. A good review of some of these models was performed by Pham et al. (2007) .

In the context of heterogeneous populations with two modes, generalizations of the Weibull distribution are recent. Saboor et al., (2019) proposed the modified beta modified-Weibull distribution with six parameters. A disadvantage of this model is that its CDF does not have a simple closed-form, it is given in terms of the beta function. Furthermore, the moment and the generating function are expressed in terms of special functions (Meijer function G) or series, which makes its applicability difficult. For heterogeneous data, a mixture of two Weibull distributions is a natural model to capture bimodality (McLachlan and Peel, 2000), however, the properties and the procedure for estimating its parameters can make its uneasy to apply. To obtain a more flexible HRF model than the Weibull model, using extended Azzalini's method (Domma, Popović, and Nadarajah, 2015), Domma et al. (2017) proposed a model called "A new

generalized weighted Weibull distribution" that has an HRF in the form decreasing, increasing, upside-down bathtub, N-shape and M-shape. However, this model remains within the class of finite mixture models, as it is a Weibull mixture model of five-component. Another model is "A new generalized odd log-logistic flexible Weibull", recently proposed by Pratavieira, et al. (2018), when considering the flexible Weibull as the G function inside generalized odd log-logistic-G (GOLL-G) class. Similar results to this were obtained by Cordeiro et al. (2021) in a LMOOLL-Weibull regression model, called "A new extended log-Weibull regression", based on the log Marshall-Olkin odd log-logistic-G (LMOOLL-G) family. In both works, the PDF can be unimodal or bimodal and the HRF can present unimodal and bathtub shapes. The mathematical properties of these models, such as moments, moment generating function, order statistics, were not included. Recently, Vila and Çankaya (2021) used a quadratic transformation technique to generate a bimodal Weibull distribution. This model is a mixture of three Weibull distributions. The CDF is expressed in terms of Gamma's incomplete function. That is, its CDF and quantile function does not have closed-forms, very useful to procedures like simulation and calculating risk measures.

In this work, we propose a new generalization of the Weibull distribution. Two models are presented, Invertible Bimodal Weibull (IBW) and it's specific case, Non-Negative Invertible Bimodal Weibull (NNIBW). The first model has either unimodal or bimodal PDF and in the second only the bimodal PDF is shown. In both models, the PDF presents various forms of asymmetry.

The CDF has a simple and invertible closed expression, so its quantile function also has a simple closed formula. This makes our model attractive to be used in simulation procedures, regression, and calculating risk measures in various areas. For example, in finance for the calculation of Value at Risk (VaR), in hydrology for the calculation of the return time (RT), and in reliability for the calculation of HRF. The HRF can take a monotonous, unimodal, bathtub, or N-shaped forms.

Furthermore, this paper is divided in 4 sections. In section 1.2, the calculation for IBW and

NNIBW models are presented along with important materials like moments, quantile function, order statistics, survival and hazard functions as well. In section 1.3, the estimation and simulation for the NNIBW model is detailed, this step generates important results for the sequence of the study. Finally, in section 1.4, the model is applied to 4 real datasets, and in one of them, is applied the regression model concluding the study.

1.2 Main Results

1.2.1 Invertible bimodal Weibull distribution

Here we propose a new generalization of the Weibull distribution using a simple method inspired by the work of Swamee and Rathei (2007). In this paper they introduce bimodality in the Normal and Log-normal distributions. This technique was also applied to generalize the logistic distributions by Rathie and Coutinho (2011). Nojosa and Rathie (2017) applied for Marshall Olkin distribution, and recently, Otiniano et al. (2021) applied to the generalized extreme value (GEV) distribution.

Given a CDF G_θ of a random variable Y; $Y \sim G_\theta$, the technique consists of composing G_θ with the function $T_{\delta,m}$, defined by

$$T_{\delta,m}(x) = (x - m)|x - m|^\delta, \ \ m \in \mathbb{R}, \ \ \delta \in [0, +\infty). \tag{1.2.1}$$

Then $G(T_{\delta,m}) = G_{\theta,\delta,m}$ is the CDF of a new random variable X, more general than Y.

For $Y \sim F_{\beta,\mu,\lambda}$, as (1.1.2), we define a random variable X, called invertible bimodal Weibull (IBW); $X \sim F_{\beta,\mu,\lambda,\delta,m}$ if

$$F_{\beta,\mu,\lambda,m,\delta}(x) = F_{\beta,\mu,\lambda}(T_{\delta,m}(x)), \tag{1.2.2}$$

where

$$T'_{\delta,m}(x) = (\delta + 1)|x - m|^\delta.$$

(1.2.3)

Since $\mu \in R$, we have two cases:

Case $\mu \geq 0$**.** By denoting $z = x - m$, the CDF and PDF of X are given, respectively, by

$$f_{\beta,\mu,\lambda,m,\delta}(z) = \begin{cases} 0, & z < \mu^{\frac{1}{\delta+1}} \\ \frac{\beta(\delta+1)}{\lambda} \exp\left\{-\left[\frac{z^{\delta+1}-\mu}{\lambda}\right]^\beta\right\} \left[\frac{z^{\delta+1}-\mu}{\lambda}\right]^{\beta-1} z^\delta, & z \geq \mu^{\frac{1}{\delta+1}}, \end{cases}$$

(1.2.4)

and

$$F_{\beta,\mu,\lambda,m,\delta}(z) = \begin{cases} 1 - \exp\left\{-\left[\frac{z^{\delta+1}-\mu}{\lambda}\right]^\beta\right\}, & z \geq \mu^{\frac{1}{\delta+1}} \\ 0, & z < \mu^{\frac{1}{\delta+1}}. \end{cases}$$

(1.2.5)

Case $\mu < 0$ **(Bimodal shapes).** The CDF and PDF of $X \sim F_{\beta,\mu,\lambda,\delta,m}$ are given, respectively, by

$$f_{\beta,\mu,\lambda,m,\delta}(z) = \begin{cases} 0, & z \leq -(-\mu)^{\frac{1}{\delta+1}} \\ \frac{\beta(\delta+1)}{\lambda} \exp\left\{-\left[\frac{-(-z)^{\delta+1}-\mu}{\lambda}\right]^\beta\right\} \left[\frac{-(-z)^{\delta+1}-\mu}{\lambda}\right]^{\beta-1} (-z)^\delta, & -(-\mu)^{\frac{1}{\delta+1}} < z < 0 \\ \frac{\beta(\delta+1)}{\lambda} \exp\left\{-\left[\frac{z^{\delta+1}-\mu}{\lambda}\right]^\beta\right\} \left[\frac{z^{\delta+1}-\mu}{\lambda}\right]^{\beta-1} z^\delta, & z \geq 0, \end{cases}$$

(1.2.6)

and

$$F_{\beta,\mu,\lambda,m,\delta} = \begin{cases} 0, & z < -(-\mu)^{\frac{1}{\delta+1}} \\ 1 - \exp\left\{ -\left[\frac{-(-z)^{\delta+1}-\mu}{\lambda} \right]^{\beta} \right\}, & -(-\mu)^{\frac{1}{\delta+1}} \leq z < 0 \\ 1 - \exp\left\{ -\left[\frac{z^{\delta+1}-\mu}{\lambda} \right]^{\beta} \right\}, & z \geq 0. \end{cases} \qquad (1.2.7)$$

Note that when $\delta = 0$ the model X becomes the base model Y; $F_{\beta,\mu,\lambda,0,m} = F_{\beta,\mu,\lambda}$. In Figures 1.1 -1.5 we show the PDF (1.2.6) and CDF (1.2.7) varying the five parameters. In the sub-figures of 1.1 and 1.2 (left), the PDF curves clearly show that m and λ are location and scale parameters, respectively. By the Figures 1.3-1.5, δ, β, and μ show to be shape parameters. The new parameter δ makes the density bimodal for values greater than zero, Figure 1.3. The modes get further apart as the value of δ grows. In the bimodal case, the β parameter influences in the asymmetry of the density and the height of the modes, Figure 1.4. When $\mu \geq 0$ the density of X is unimodal, while for $\mu < 0$ the density is bimodal. For that reason, here we illustrate the density curves for $\mu < 0$. The sub-figures on the right show a CDF with variations of concave and convex shapes and mixtures between them.
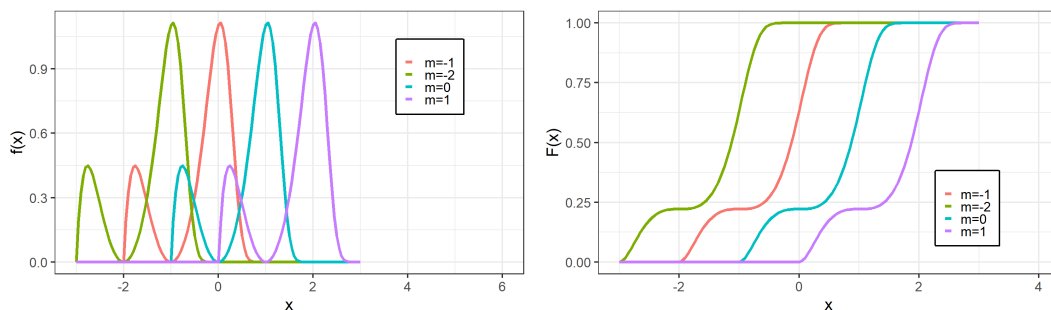

Figure 1.1: m variation in $X \sim F_{2,-1,2,2,m}$: PDF(left) and CDF (right).
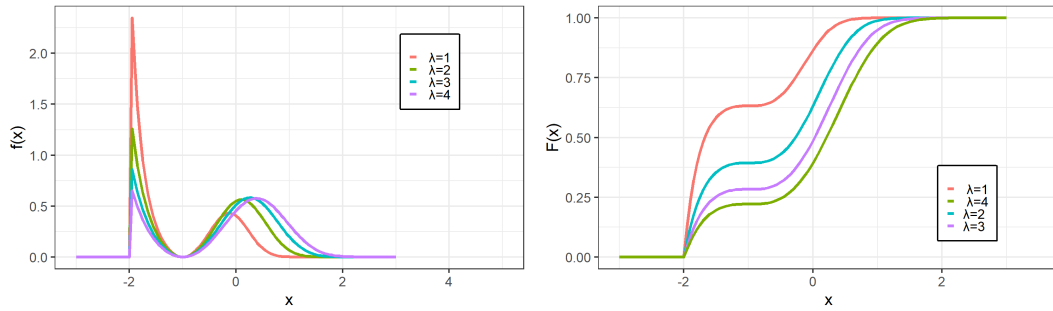
Figure 1.2: λ variation in $X \sim F_{1,-1,\lambda,2,-1}$: PDF(left) and CDF (right).
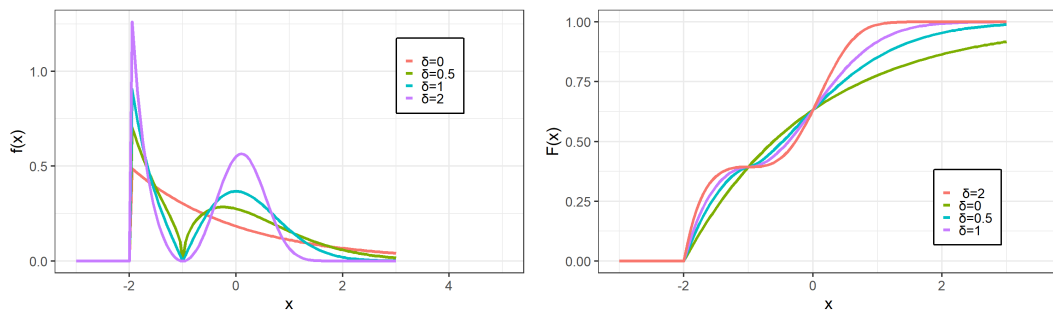

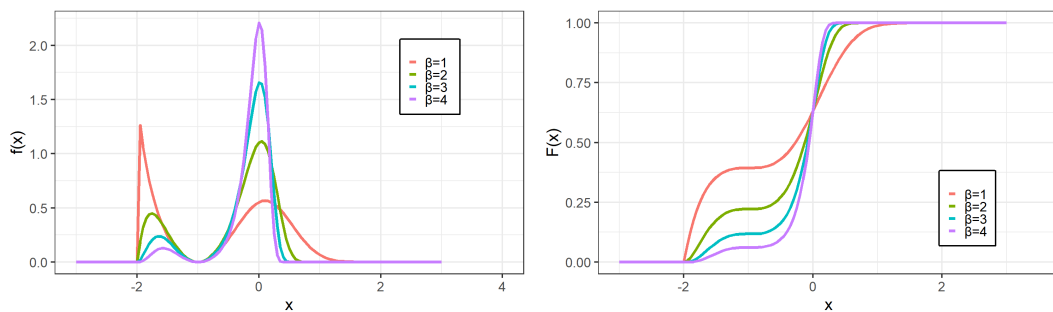**Figure 1.3:** δ variation in $X \sim F_{1,-1,2,\delta,-1}$: PDF(left) and CDF (right).

Figure 1.4: β variation in $X \sim F_{\beta,-1,2,2,-1}$: PDF(left) and CDF (right).
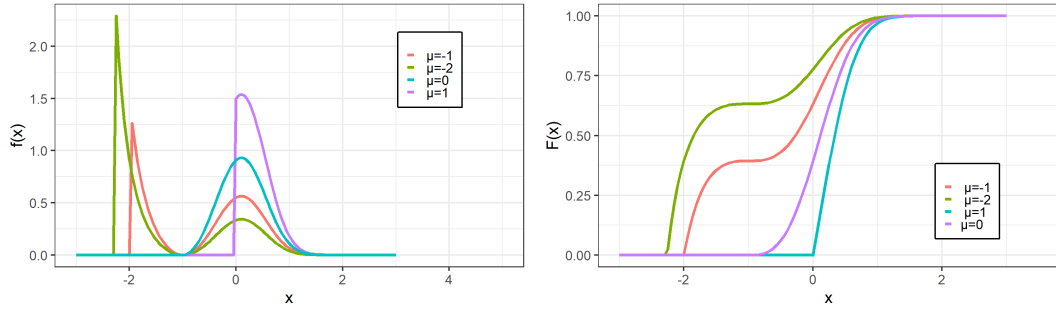
Figure 1.5: μ variation in $X \sim F_{1,\mu,1,2,-1}$: PDF(left) and CDF (right).

Mode

The PDF of a random variable $X \sim F_{\beta,\mu,\lambda,\delta,m}$ can be unimodal or bimodal.

Proposition 1.2.1. *A real value x_m is a mode point of $f_{\beta,\mu,\lambda,m,\delta}$ if it is a solution to the equation*

$$T_{\delta,m}{}''(x) + (\beta - 1)(T_{\delta,m}(x) - \mu)^{-1} - \frac{\beta}{\lambda^\beta}(T_{\delta,m}(x) - \mu)^{\beta-1} = 0, \qquad (1.2.8)$$

where $T_{\delta,m}(x)$ is given in (1.2.1), $T_{\delta,m}''(x) = \delta(\delta + 1)\mathrm{sgn}(x - m)|x - m|^{\delta-1}$, and $\mathrm{sgn}(t) = \frac{t}{|t|}$.

Proof. The proof proceeds directly by computing the critical points of the function (1.2.6) . $\square$

Moments

The moments of a random variable X are important descriptive measures of populations. To calculate the moments of a random variable $X \sim F_{\beta,\mu,\lambda,\delta,0}$ here we use the gamma function, upper incomplete gamma function, and lower incomplete gamma function, given, respectively, by

$$\Gamma(a) = \int_0^{+\infty} t^{a-1}e^{-t}dt, \qquad (1.2.9)$$

$$\Gamma(a;x) = \int_0^x t^{a-1}e^{-t}dt, \qquad (1.2.10)$$

and

$$\gamma(a; x) = \int_x^\infty t^{a-1} e^{-t} dt. \tag{1.2.11}$$

Proposition 1.2.2. *Let $X \sim F_{\beta,\mu,\lambda,\delta,0}$ and $r \in \mathbb{N}$. We have that if $\mu > 0$, then*

$$E(X^{r(\delta+1)}) = \sum_{k=0}^{r} \binom{r}{k} \lambda^{r-k} \mu^k \, \Gamma\left(\frac{r-k}{\beta} + 1\right) \tag{1.2.12}$$

and if $\mu \le 0$, then

$$
\begin{aligned}
E(X^{r(\delta+1)}) &= (-1)^{r(\delta+1)} \sum_{k=0}^{r} \binom{r}{k} (-\mu)^k \lambda^{r-k} \Gamma\left(\frac{r-k}{\beta} + 1; \left(-\frac{\mu}{\lambda}\right)^\beta\right) \\
&+ \sum_{k=0}^{r} \binom{r}{k} \mu^k \gamma\left(\frac{r-k}{\beta} + 1; \left(\frac{-\mu}{\lambda}\right)^\beta\right).
\end{aligned} \tag{1.2.13}
$$

Proof. By definition, for $\mu > 0$, we have

$$E(X^{r(\delta+1)}) = \int_{(\mu)^{\frac{1}{\delta+1}}}^{+\infty} x^{r(\delta+1)} \frac{\beta(\delta+1)}{\lambda} \exp\left\{-\left[\frac{x^{\delta+1}-\mu}{\lambda}\right]^\beta\right\} \left[\frac{x^{\delta+1}-\mu}{\lambda}\right]^{\beta-1} x^\delta dx \tag{1.2.14}$$

and for $\mu \le 0$

$$
\begin{aligned}
E\left(X^{r(\delta+1)}\right) &= \int_{-(-\mu)^{\frac{1}{\delta+1}}}^{0} x^{r(\delta+1)} \frac{\beta(\delta+1)}{\lambda} \exp\left\{-\left[\frac{-(-x)^{\delta+1}-\mu}{\lambda}\right]^\beta\right\} \left[\frac{-(-x)^{\delta+1}-\mu}{\lambda}\right]^{\beta-1} (-x)^\delta dx \\
&+ \int_{0}^{\infty} x^{r(\delta+1)} \frac{\beta(\delta+1)}{\lambda} \exp\left\{-\left[\frac{x^{\delta+1}-\mu}{\lambda}\right]^\beta\right\} \left[\frac{x^{\delta+1}-\mu}{\lambda}\right]^{\beta-1} x^\delta dx.
\end{aligned} \tag{1.2.15}
$$

For the positive integrals of (1.2.14) and (1.2.15) we use the substitution $y = \left[\frac{x^{\delta+1}-\mu}{\lambda}\right]^\beta$ and for the negative integral of (1.2.15) we use the substitution $y = \left[\frac{-(-x)^{\delta+1}-\mu}{\lambda}\right]^\beta$. Thus, with some algebraic manipulations and application of Newton's binomial formula, we update (1.2.14) and

(1.2.15), respectively, by

$$E(X^{r(\delta+1)}) = \sum_{k=0}^{r} \binom{r}{k} \lambda^{r-k} \mu^k \int_0^{+\infty} y^{\frac{r-k}{\beta}} e^{-y} dy \qquad (1.2.16)$$

and

$$
\begin{aligned}
E\left(x^{r(\delta+1)}\right) &= (-1)^{r(\delta+1)} \sum_{k=0}^{r} \binom{r}{k} (-\mu)^k \lambda^{r-k} \int_0^{\left(-\frac{\mu}{\lambda}\right)^\beta} y^{\frac{r-k}{\beta}} e^{-y} dy \\
&+ \sum_{k=0}^{r} \binom{r}{k} \mu^k \int_{\left(-\frac{\mu}{\lambda}\right)^\beta}^{\infty} y^{\frac{r-k}{\beta}} e^{-y} dy.
\end{aligned}
\qquad (1.2.17)
$$

The proof is completed by expressing the integrals (1.2.16) and (1.2.17) in terms of the gamma functions (1.2.9)-(1.2.11).

$\square$

Quantile function

In hydrology and environmental data, the interest is the estimation of the probability of a given process giving a value that exceeds a given level z in a future period. The T period (or return time) of return level z is the expected waiting time until z is next exceeded. For independent and identically distributed processes, return level and return periods correspond to quantiles and exceedance probabilities, respectively.

If

$$P(X > z_p) = 1 - F(z_p)$$

$$= p$$

and $T = \frac{1}{p}$, then the return level

$$z_p = F^{-1}\left(1 - \frac{1}{T}\right) \qquad (1.2.18)$$

has return period $p^{-1} = T$.

For the random variable $X \sim F_{\beta,\mu,\lambda,\delta,m}$ with $\mu < 0$, the $1/p$ level z_p is the $1 - p$ quantile of the invertible bimodal Weibull (IBW) distribution for $0 < p < 1$.

$$z_p = \begin{cases} \left[\mu + \lambda[-\ln(p)]^{\frac{1}{\beta}}\right]^{\frac{1}{\delta+1}} + m, & p \leq \exp\left[-\left(-\frac{\mu}{\lambda}\right)^{\beta}\right] \\ -\left[-\mu - \lambda[-\ln(p)]^{\frac{1}{\beta}}\right]^{\frac{1}{\delta+1}} + m, & p > \exp\left[-\left(-\frac{\mu}{\lambda}\right)^{\beta}\right]. \end{cases} \tag{1.2.19}$$

To calculate z_p just consider the CDF (1.2.7) and the inverse function

$$\begin{aligned} T_{\delta,m}^{-1}(t) &= \text{sgn(t)}|\text{t}|^{\frac{1}{\delta+1}} + \text{m} \\ &= \begin{cases} t^{\frac{1}{\delta+1}} + m, & t \geq 0 \\ -(-t)^{\frac{1}{\delta+1}} + m, & t < 0. \end{cases} \end{aligned} \tag{1.2.20}$$

This function is also used to generate random samples of X, using the inverse transformation method.

Order Statistics

Given a random sample of X of size N; $X_1, \ldots, X_n$ independent and identically distributed (iid) random variables. If re-ordering them $X_{(1)} < X_{(2)} < \ldots < X_{(n)}$ then $X_{(i)}$ is called the i-th order statistic. The smallest order statistic and the largest order statistic are $X_{(1)} = \min\{X_1, \ldots, X_n\}$ and $X_{(n)} = \max\{X_1, \ldots, X_n\}$, respectively. The extreme value theory is based on the study of the asymptotic distribution of $X_{(1)}$ and $X_{(n)}$, however the exact distribution of the i-th order statistic can be useful in several applications (Seber and Lee, 2003).

Proposition 1.2.3. *Let* $X \sim F_{\beta,\mu,\lambda,\delta,m}$ *then the PDF of i-th order statistic of the sample*

$X_1, \ldots, X_n$ *is give by*

$$f_{(i)}(x) = \frac{n!}{(i-1)!(n-i)!} \frac{\beta}{\lambda} \exp\left[-(n-i+1)\left(\frac{T(x)-\mu}{\lambda}\right)^{\beta}\right] \left(\frac{T(x)-\mu}{\lambda}\right)^{\beta-1}$$

$$* \left\{1 - \exp\left[-\left(\frac{T(x)-\mu}{\lambda}\right)^{\beta}\right]\right\},$$

for $x > T_{\delta,m}^{-1}(\mu)$, where $T_{\delta,m}$ and $T_{\delta,m}^{-1}$ are given in (1.2.1) and (1.2.20), respectively.

Proof. The proof follows directly from the function (1.2.2) and its derivative. $\square$

1.2.2 Non-negative invertible bimodal Weibull distribution

Here, the random variable $X \sim F_{\beta,\mu,\lambda,\delta,m}$ of (1.2.7) is reparameterized by making $m = (-\mu)^{\frac{1}{\delta+1}}$, then the new random variable $X \sim F_{\text{NNIBW}}(.;\boldsymbol{\theta})$ is non-negative and $\boldsymbol{\theta} = (\beta, \mu, \lambda, \delta)$ is the vector of parameters. When considering $v = x - (-\mu)^{\frac{1}{\delta+1}}$, the CDF F_{NNIBW} is given by

$$F_{\text{NNIBW}}(x;\boldsymbol{\theta}) = \begin{cases} 0, & v \leq -(-\mu)^{\frac{1}{\delta+1}} \\ 1 - \exp\left\{-\left[\frac{-(-v)^{\delta+1}-\mu}{\lambda}\right]^{\beta}\right\}, & -(-\mu)^{\frac{1}{\delta+1}} < v < 0 \\ 1 - \exp\left\{-\left[\frac{v^{\delta+1}-\mu}{\lambda}\right]^{\beta}\right\}, & v \geq 0, \end{cases} \quad (1.2.21)$$

Using the indicator function on the range A,

$$I_A(x) = \begin{cases} 1, & \text{if } x \in A \\ 0, & \text{if } x \notin A, \end{cases}$$

the corresponding PDF is written as

$$f_{\text{NNIBW}}(x;\boldsymbol{\theta}) = f_1(x;\boldsymbol{\theta})I(x)_{[0,(-\mu)^{\frac{1}{\delta+1}}]} + f_2(x;\boldsymbol{\theta})I(x)_{[(-\mu)^{\frac{1}{\delta+1}},+\infty]} \quad (1.2.22)$$
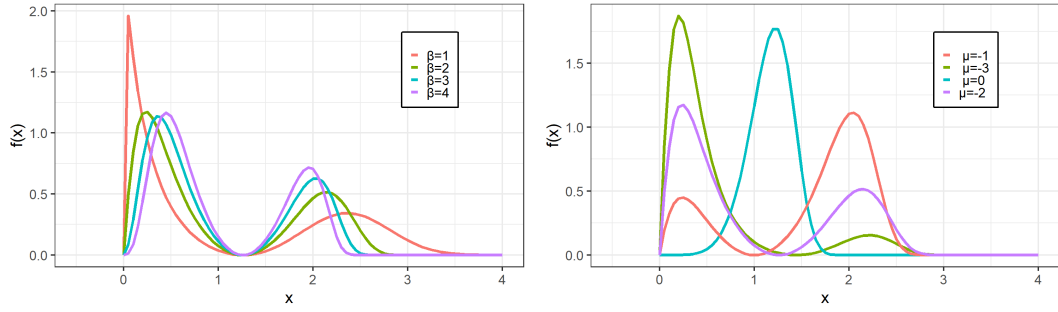
Figure 1.6: PDF of $X \sim F_{\mathrm{NNIBW}}(.; \beta, -2, 2, 2)$ (left) and PDF of $X \sim F_{\mathrm{NNIBW}}(.; 2, \mu, 1, 2)$(right).
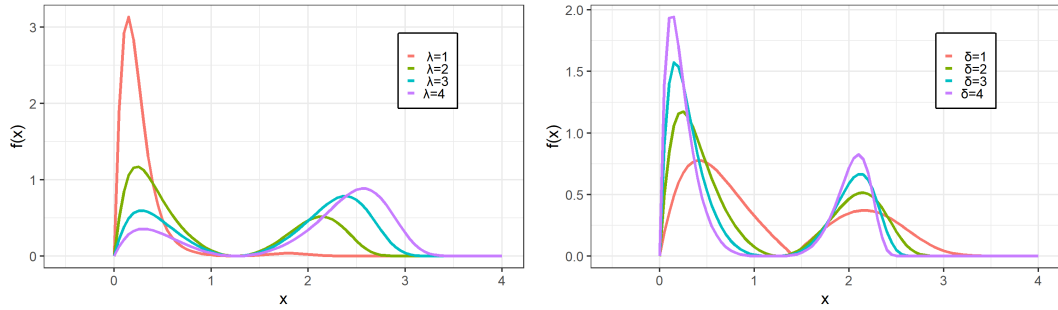
Figure 1.7: PDF of $X \sim F_{\mathrm{NNIBW}}(.; 2, -2, \lambda, 2)$ (left) and PDF of $X \sim F_{\mathrm{NNIBW}}(.; 2, -2, 2, \delta)$(right)

where

$$f_1(x; \boldsymbol{\theta}) = \frac{\beta(\delta+1)}{\lambda} \exp\left\{ -\left[\frac{-(-v)^{\delta+1} - \mu}{\lambda} \right]^{\beta} \right\} \left[\frac{-(-v)^{\delta+1} - \mu}{\lambda} \right]^{\beta-1} (-v)^{\delta} \quad (1.2.23)$$

and

$$f_2(x; \boldsymbol{\theta}) = \frac{\beta(\delta+1)}{\lambda} \exp\left\{ -\left[\frac{v^{\delta+1} - \mu}{\lambda} \right]^{\beta} \right\} \left[\frac{v^{\delta+1} - \mu}{\lambda} \right]^{\beta-1} v^{\delta}. \quad (1.2.24)$$

The different formats of the PDF of $X \sim F_{\mathrm{NNIBW}}(.; \boldsymbol{\theta})$ are shown in Figures 1.9 and 1.7. In this case, the λ parameter is also a shape parameter.

The survival function and the HRF are very useful functions in reliability applications.

These functions, for $X \sim F_{\mathrm{NNIBW}}(.;\boldsymbol{\theta})$, are given, respectively, by

$$
S_{\mathrm{NNIBW}}(x;\boldsymbol{\theta}) = \begin{cases} 1, & v < -(-\mu)^{\frac{1}{\delta+1}} \\ \exp\left\{ -\left[\frac{-(-v)^{\delta+1}-\mu}{\lambda}\right]^{\beta} \right\}, & -(-\mu)^{\frac{1}{\delta+1}} \leq v < 0 \\ \exp\left\{ -\left[\frac{v^{\delta+1}-\mu}{\lambda}\right]^{\beta} \right\}, & v \geq 0 \end{cases} \tag{1.2.25}
$$

and

$$
h_{\mathrm{NNIBW}}(x;\boldsymbol{\theta}) = \begin{cases} 0, & v < -(-\mu)^{\frac{1}{\delta+1}} \\ \frac{\beta(\delta+1)}{\lambda}\left[\frac{-(-v)^{\delta+1}-\mu}{\lambda}\right]^{\beta-1}(-v)^{\delta}, & -(-\mu)^{\frac{1}{\delta+1}} \leq v < 0 \\ \frac{\beta(\delta+1)}{\lambda}\left[\frac{v^{\delta+1}-\mu}{\lambda}\right]^{\beta-1}v^{\delta}, & v \geq 0 \end{cases} \tag{1.2.26}
$$

Figure 1.8 shows the well-known HRF of $X \sim F_{\mathrm{NNIBW}}(.;\beta,\mu,\lambda,0) = F_{\beta,\lambda,\mu}$ (three-parameter Weibull (1.1.2)). Figure 1.9 shows a more flexible HRF of $X \sim F_{\mathrm{NNIBW}}(.;\beta,\mu,\lambda,\delta)$. It depends on the variations of the parameters $\beta, \mu, \lambda,$ and δ.
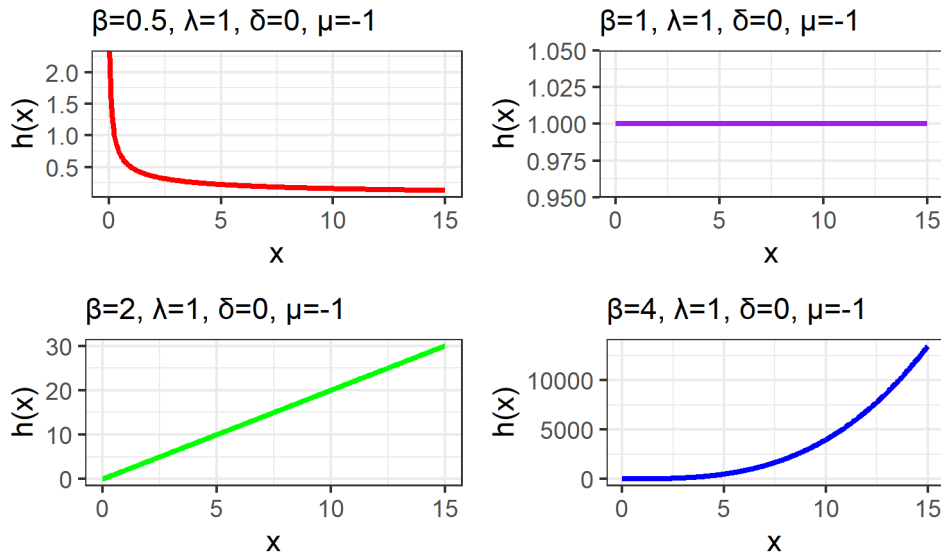
Figure 1.8: HRF curve of $X \sim F_{\mathrm{NNIBW}}(.;\beta,\mu,\lambda,\delta)$ for $\delta = 0$ and varying β.
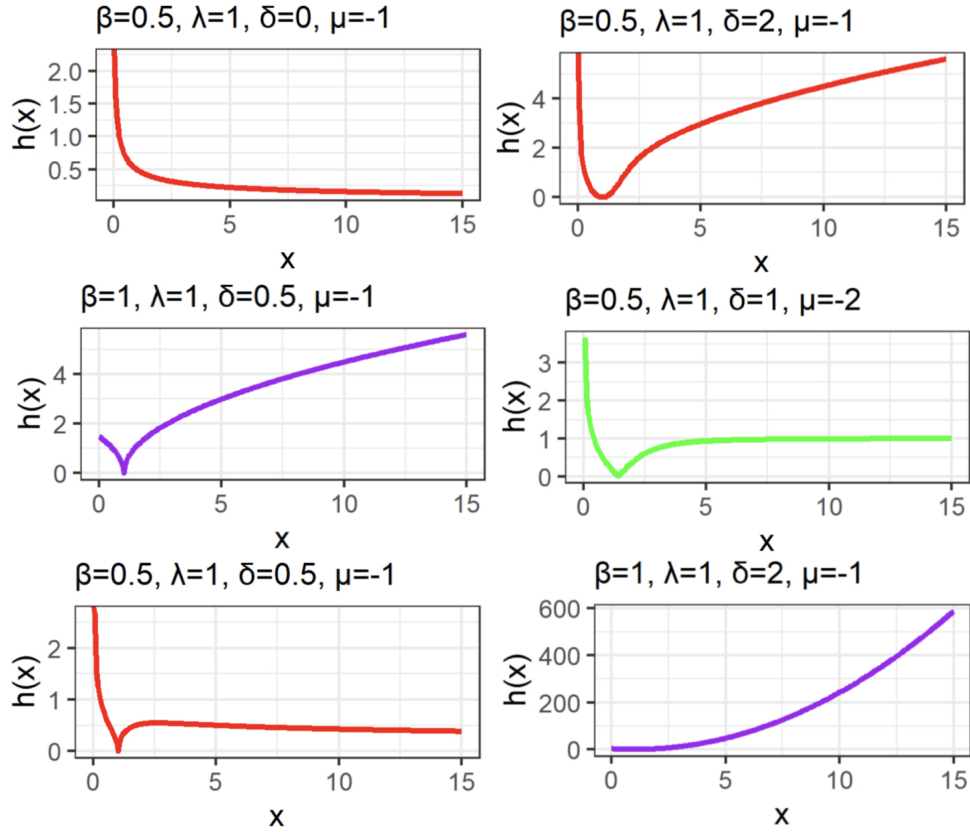
Figure 1.9: HRF curve of $X \sim F_{\text{NNIBW}}(.; \beta, \mu, \lambda, \delta)$ for the legend parameters.

1.3 Estimation and Simulation

1.3.1 Maximum likelihood estimation

We consider maximum likelihood estimates (MLE) of the unknown parameters $\boldsymbol{\theta} = (\beta, \mu, \lambda, \delta)$ that appear in the NNIBW model with PDF (1.2.22). Supposing that $(x_1, x_2, \ldots, x_n)$ are the values of a random sample of $X \sim F_{\text{NNIBW}}(.; \boldsymbol{\theta})$, then the corresponding log-likelihood function is

$$
\begin{aligned}
l(\boldsymbol{\theta} \mid x) &= \sum_{i=1}^{n} \log[f_{\text{NNIBW}}(x_i; \boldsymbol{\theta})] \\
&= l_1(\boldsymbol{\theta} \mid x) + l_2(\boldsymbol{\theta} \mid x).
\end{aligned} \tag{1.3.1}
$$

Without loss of generality, assume that the sample is given by $(x_1, \ldots, x_k, x_{k+1}, \ldots, x_n)$, in which $x_i < (-\mu)^{\frac{1}{\delta+1}}$ for $i = 1, \ldots, k$ and $x_i \geq (-\mu)^{\frac{1}{\delta+1}}$ for $i = k+1, \ldots, n$, then the expressions of $l_1(\boldsymbol{\theta} \mid x)$ and $l_2(\boldsymbol{\theta} \mid x)$ of (1.3.1) are given by

$$l_1(\boldsymbol{\theta} \mid x) = \sum_{i=1}^{k} \log \left[f_1(x_i; \boldsymbol{\theta}) I_{\left(0, (-\mu)^{\frac{1}{\delta+1}}\right)}(x_i) \right]$$

$$\text{and} \qquad (1.3.2)$$

$$l_2(\boldsymbol{\theta} \mid x) = \sum_{i=k+1}^{n} \log \left[f_2(x_i; \boldsymbol{\theta}) I_{\left[(-\mu)^{\frac{1}{\delta+1}}, +\infty\right)}(x_i) \right],$$

where, using the notation $v_i = x_i - (-\mu)^{\frac{1}{1+\delta}}$, one has that

$$\log f_1(x_i; \boldsymbol{\theta}) = \log(\beta) + \log(\delta+1) - \log(\lambda) - \left[\frac{-(-v_i)^{\delta+1} - \mu}{\lambda} \right]^{\beta}$$

$$+ (\beta - 1) \log \left[\frac{-(-v_i)^{\delta+1} - \mu}{\lambda} \right] + \delta \log(-v_i)$$

and

$$\log f_2(x_i; \boldsymbol{\theta}) = \log(\beta) + \log(\delta+1) - \log(\lambda) - \left[\frac{v_i^{\delta+1} - \mu}{\lambda} \right]^{\beta} + (\beta - 1) \log \left[\frac{v_i^{\delta+1} - \mu}{\lambda} \right] + \delta \log v_i.$$

$$(1.3.3)$$

By combining the functions (1.3.2)-(1.3.3) into (1.3.1), the log-likelihood function results in

$$l(\boldsymbol{\theta} \mid x) = n \log(\beta) + n \log(\delta + 1) - n \log(\lambda)$$

$$- \sum_{i=1}^{k} (\Psi_i^1)^{\beta} + (\beta - 1) \sum_{i=1}^{k} \log \Psi_i^1 + \delta \sum_{i=1}^{k} \log(-v_i)$$

$$- \sum_{i=k+1}^{n} (\Psi_i^2)^{\beta} + (\beta - 1) \sum_{i=k+1}^{n} \log \Psi_i^2 + \delta \sum_{i=k+1}^{n} \log(v_i) \qquad (1.3.4)$$

where $\Psi_i^1 = \frac{-(-v_i)^{\delta+1} - \mu}{\lambda}$ and $\Psi_i^2 = \frac{v_i^{\delta+1} - \mu}{\lambda}$. As

$$\frac{\partial}{\partial \mu} \Psi_i^1 = \frac{1}{\lambda} \left[(-v_i)^{\delta} (-\mu)^{-\frac{1}{\delta+1}} - 1 \right],$$

$$\frac{\partial}{\partial \mu} \Psi_i^2 = \frac{1}{\lambda} \left[(v_i)^{\delta} (-\mu)^{-\frac{\delta}{\delta+1}} - 1 \right]$$

$$\frac{\partial}{\partial \lambda} \Psi_i^1 = -\frac{1}{\lambda} \Psi_i^1,$$

$$\frac{\partial}{\partial \lambda} \Psi_i^2 = -\frac{1}{\lambda} \Psi_i^2$$

$$\frac{\partial}{\partial \delta} \Psi_i^1 = -\frac{1}{\lambda} \left[(-v_i)^{\delta+1} \log(-v_i) + (\delta + 1)^{-1} (-v_i)^{\delta} (-\mu)^{\frac{1}{\delta+1}} \log(-\mu) \right],$$

$$\frac{\partial}{\partial \delta} \Psi_i^2 = \frac{1}{\lambda} \left[(v_i)^{\delta+1} \log(v_i) + (\delta + 1)^{-1} (v_i)^{\delta} (-\mu)^{\frac{1}{\delta+1}} \log(-\mu) \right]$$

Then, the maximum likelihood estimates of λ, β, μ, and δ are solutions of the following system of equations

$$\frac{\partial l(\boldsymbol{\theta} \mid x)}{\partial \lambda} = \frac{-n\beta}{\lambda} + \frac{\beta}{\lambda} \sum_{i=1}^{k} (\Psi_i^1)^{\beta} + \frac{\beta}{\lambda} \sum_{i=k+1}^{n} (\Psi_i^2)^{\beta} = 0; \qquad (1.3.5)$$

$$\frac{\partial l(\boldsymbol{\theta} \mid x)}{\partial \beta} = \frac{n}{\beta} - \sum_{i=1}^{k} (\Psi_i^1)^\beta \log(\Psi_i^1) + \sum_{i=1}^{k} \log(\Psi_i^1) \tag{1.3.6}$$
$$- \sum_{i=k+1}^{n} (\Psi_i^2)^\beta \log(\Psi_i^2) + \sum_{i=k+1}^{n} \log(\Psi_i^2) = 0;$$

$$\begin{aligned}
\frac{\partial \ell(\boldsymbol{\theta}|x)}{\partial \mu} &= -\frac{\beta}{\lambda} \sum_{i=1}^{k} (\Psi_i^1)^{\beta-1} \left[(-\mu)^{-\frac{\delta}{\delta+1}} (-v_i)^\delta - 1 \right] + \frac{(\beta-1)}{\lambda} \sum_{i=1}^{k} (\Psi_i^1)^{-1} \left[(-\mu)^{-\frac{\delta}{\delta+1}} (-v_i)^\delta - 1 \right] \\
&\quad - \frac{\beta}{\lambda} \sum_{i=k+1}^{n} (\Psi_i^2)^{\beta-1} \left[(-\mu)^{-\frac{\delta}{\delta+1}} v_i^\delta - 1 \right] + \frac{(\beta-1)}{\lambda} \sum_{i=k+1}^{n} (\Psi_i^2)^{-1} \left[(-\mu)^{-\frac{\delta}{\delta+1}} v_i^\delta - 1 \right] \\
&\quad - \frac{\delta}{\delta+1} (-\mu)^{-\frac{\delta}{1+\delta}} \sum_{i=k+1}^{n} (-v_i)^{-1} + \frac{\delta}{\delta+1} (-\mu)^{-\frac{\delta}{1+\delta}} \sum_{i=k+1}^{n} (v_i)^{-1} = 0; \tag{1.3.7}
\end{aligned}$$

$$\begin{aligned}
\frac{\partial l(\boldsymbol{\theta}|x)}{\partial \delta} &= \sum_{i=1}^{k} \left(\frac{\beta}{\lambda} (\Psi_i^1)^{\beta-1} - \frac{(\beta-1)}{\lambda} (\Psi_i^1)^{-1} \right) \left[(-v_i)^{\delta+1} \log(-v_i) + (\delta+1)^{-1} (-v_i)^\delta (-\mu)^{\frac{1}{\delta+1}} \log(-\mu) \right] \\
&\quad - \frac{\beta}{\lambda} \sum_{i=k+1}^{n} \left(\frac{\beta}{\lambda} (\Psi_i^2)^{\beta-1} - \frac{(\beta-1)}{\lambda} (\Psi_i^2)^{-1} \right) \left[(v_i)^{\delta+1} \log(v_i) + (\delta+1)^{-1} (v_i)^\delta (-\mu)^{\frac{1}{\delta+1}} \log(-\mu) \right] \\
&\quad + \frac{n}{\delta+1} - \frac{\delta}{(\delta+1)^2} (-\mu)^{\frac{\delta}{\delta+1}} \log(-\mu) \sum_{i=1}^{k} v_i^{-1} \\
&\quad + \frac{\delta}{(\delta+1)^2} (-\mu)^{\frac{1}{\delta+1}} \log(-\mu) \sum_{i=k+1}^{n} v_i^{-1} = 0. \tag{1.3.8}
\end{aligned}$$

1.3.2 MLE performance via simulation

As the initial idea was to apply data to the survival model, the NNIBW function was used for the simulation and for the applications. To test the performance of maximum likelihood estimation of λ, β, μ, and δ, via Monte Carlo simulation, here we proceed as follows: First, we draw fourteen vectors of parameters $\boldsymbol{\theta}$ of $X \sim F_{\text{NNIBW}}(.; \boldsymbol{\theta})$, then we simulate samples of various

sizes for each $X \sim F_{\text{NNIBW}}(.;\boldsymbol{\theta}_\ell)$, $\ell = 1,\dots,14$. Finally, after maximizing the function (1.3.4), we obtain the mean estimates and their mean squared error (MSE). The fourteen vectors of the $\boldsymbol{\theta}_\ell$ are the combination of the following values: $\beta = 1,2$, $\lambda = 1,2$, $\delta = 0.5,1$ and $\mu = -1,-2$. The parameters set are detailed in the third column of Tables 1.1 and 1.2.

The procedures for simulating X and calculating maximum likelihood estimates were implemented in the Project for Statistical Computing, R-4.0.5 for Windows. The quantile function, determined in section 1.2, was essential to apply the inverse transformation method to generate the random samples of X, because for a random sample $p \sim U(0,1)$ just apply (1.2.19). So, we use the following procedure:

(i) Generate M=1000 random samples from $X \sim F_{NNWBI}(.;\boldsymbol{\theta})$, $\boldsymbol{\theta} = (\beta,\delta,\mu,\lambda)$, using (1.2.19), of size $N = 50,100,500$.

(ii) Optimizing (1.3.4) with "optim" library in R, then calculate the mean estimate $\hat{\boldsymbol{\theta}} = \frac{1}{M}\sum_{i=1}^{M}\hat{\boldsymbol{\theta}}_i$ and the $\text{MSE}(\hat{\boldsymbol{\theta}}) = \frac{1}{M}\sum_{i=1}^{M}(\hat{\boldsymbol{\theta}}_i - \boldsymbol{\theta})^2$.

(iii) For the initial value, consider the actual parameter value plus a random value from the random variable $U(0,1)$.

The results of the mean estimate of $\boldsymbol{\theta}$ and $\text{MSE}(\hat{\boldsymbol{\theta}})$ are in Tables 1.1 and 1.2. Note that as the sample size grows (N=50 to 500), the MSE value decreases. This explains the convergence of the estimator $\hat{\boldsymbol{\theta}}$ to $\boldsymbol{\theta}$.

The good performance of the maximum likelihood estimator $\hat{\boldsymbol{\theta}}$ is also illustrated in the Appendix A, Figures 24-30. In these figures, we compare the fitted values from a sample of sizes 50 and 500 with the theoretical density adjusted to the values of parameters in Tables 1.1 and 1.2. In these figures, it can be observed that the values are close to the real density, and as the size of sample increase, the fitted values get even closer. This is an indication of the good performance of the obtained maximum likelihood estimates.

Table 1.1: Mean estimates and its MSE for θ_1 to θ_7

		θ	N_{50}	N_{100}	N_{500}	EQM_{50}	EQM_{100}	EQM_{500}
	β	1	1.046	1.019	1.003	0.019	0.007	0.001
θ_1	λ	1	1.031	1.018	1.002	0.03	0.014	0.003
	δ	0.5	0.604	0.551	0.509	0.065	0.025	0.005
	μ	-1	-1.058	-1.026	-1.004	0.045	0.013	0.001
	β	2	2.156	2.074	2.016	0.134	0.046	0.007
θ_2	λ	1	1.013	1.01	1.002	0.007	0.003	0.001
	δ	0.5	0.6	0.543	0.509	0.057	0.023	0.004
	μ	-1	-1.022	-1.016	-1.002	0.012	0.005	0
	β	1	1.029	1.015	1.003	0.018	0.008	0.001
θ_3	λ	2	2.075	2.032	2.003	0.126	0.056	0.01
	δ	0.5	0.562	0.53	0.506	0.046	0.021	0.003
	μ	-1	-1.051	-1.023	-1.005	0.051	0.015	0.001
	β	2	2.078	2.021	2.002	0.094	0.035	0.007
θ_4	λ	2	2.023	2.007	2.003	0.028	0.014	0.002
	δ	0.5	0.548	0.529	0.507	0.043	0.018	0.003
	μ	-1	-1.018	-1.01	-1.002	0.021	0.007	0.001
	β	1	1.05	1.022	1.005	0.02	0.008	0.001
θ_5	λ	1	1.024	1.018	1.001	0.03	0.014	0.003
	δ	1	1.122	1.067	1.01	0.109	0.048	0.008
	μ	-1	-1.031	-1.017	-1.003	0.028	0.012	0.001
	β	2	2.154	2.058	2.008	0.153	0.049	0.007
θ_6	λ	1	1.007	1.004	1	0.009	0.004	0.001
	δ	1	1.113	1.05	1.007	0.098	0.042	0.007
	μ	-1	-1.012	-1.004	-1.002	0.01	0.004	0.001
	β	1	1.031	1.012	0.999	0.021	0.008	0.001
θ_7	λ	2	2.079	2.035	2.009	0.151	0.058	0.011
	δ	1	1.093	1.04	1.012	0.08	0.034	0.006
	μ	-1	-1.037	-1.007	-1.002	0.035	0.011	0.002

Table 1.2: Mean estimates and its MSE for θ_7 to θ_{14}

		θ	N_{50}	N_{100}	N_{500}	EQM_{50}	EQM_{100}	EQM_{500}
	β	2	2.059	2.039	2.004	0.102	0.042	0.007
	λ	2	2.018	2.009	2.003	0.031	0.013	0.002
θ_8	δ	1	1.064	1.021	1.009	0.07	0.029	0.006
	μ	-1	-1.007	-1.008	-1.001	0.02	0.008	0.001
	β	1	1.072	1.028	1.005	0.027	0.011	0.002
	λ	1	1.173	1.074	1.009	0.165	0.061	0.008
θ_9	δ	0.5	0.663	0.573	0.509	0.139	0.058	0.008
	μ	-2	-2.26	-2.132	-2.015	0.459	0.15	0.012
	β	1	1.043	1.02	1.004	0.019	0.007	0.001
	λ	2	2.183	2.074	2.02	0.272	0.092	0.018
θ_{10}	δ	0.5	0.606	0.543	0.511	0.065	0.025	0.004
	μ	-2	-2.19	-2.074	-2.022	0.252	0.064	0.008
	β	2	2.156	2.075	2.013	0.148	0.053	0.007
	λ	2	2.131	2.056	2.008	0.12	0.041	0.007
θ_{11}	δ	0.5	0.596	0.546	0.505	0.056	0.023	0.004
	μ	-2	-2.138	-2.059	-2.008	0.132	0.035	0.005
	β	1	1.065	1.027	1.006	0.03	0.011	0.002
	λ	1	1.171	1.063	1.012	0.229	0.061	0.008
θ_{12}	δ	1	1.192	1.076	1.019	0.264	0.095	0.015
	μ	-2	-2.26	-2.101	-2.017	0.564	0.138	0.015
	β	1	1.041	1.019	1.005	0.019	0.008	0.001
	λ	2	2.181	2.076	2.014	0.27	0.111	0.018
θ_{13}	δ	1	1.109	1.057	1.01	0.105	0.044	0.008
	μ	-2	-2.159	-2.077	-2.016	0.232	0.079	0.01
	β	2	2.149	2.072	2.01	0.147	0.058	0.008
	λ	2	2.117	2.06	2.007	0.114	0.053	0.008
θ_{14}	δ	1	1.117	1.055	1.007	0.099	0.048	0.007
	μ	-2	-2.12	-2.058	-2.008	0.121	0.052	0.006

1.4   Applications

The four temperature data sets used in the application of our model correspond to the localities of Svalbard Islands(NO), Delhi(IN), Dawson City (CA), and Yellowknife (CA).

Svalbard is a Norwegian archipelago. The geographical location is illustrated in Figure 1.10, the archipelago has an arctic climate and the average temperature varies between 4 °C and 7 °C in summer (from June to September) and -13 °C and -9 °C in winter (from December to March). The data is freely available on *kaggle* plataform (*Svalbard Climate, 1910-2017* 2022), it consists of the monthly average temperature for the years 1912 to 2017 from January to December, that is 1720 observations for the temperature.

Figure 1.10: Geographical location of Svalbard Island as https://www.bing.com/images.

Delhi is located in northern India, see, Figure 1.11. Delhi's climate is humid subtropical, where summer are usually long and hot and winter are mild and short. The average annual temperature is of 25 °C . In summer, the temperature varies between 29 °C and 33 °C (from April to July), while in winter, the temperature varies between 14 °C and 17 °C (from August to March). The data was also obtained in *kaggle* plataform (*Daily Climate time series data* 2022) and it consists of the average daily temperature of 2017 in the period from January 1st to April 24th, that is 114 observations.

Figure 1.11: Geographical location of Delhi as https://www.bing.com/images.

Dawson City and Yellowknife are sub-Arctic Canadian cities, Figure 1.12, with positive average temperatures from June to September and negatives from December to March. The data for Dawson City corresponds to the maximum of daily temperature in the year of 2021, that is a little less than 365 observations, due to some missing data. On the other hand, for the Yellowknife, Initially, the minimum daily temperatures from January 1953 to August 2022 were considered. To decrease the temporal dependence of the data, we used the technique of minimum blocks of size 90 and obtained a sub-sample of 281 data. Both datasets were obtained at the official website for climate data from Canada's government (*Climate Weather* 2022).

Figure 1.12: Geographical location of Dawson City and Yellowknife as https://www.bing.com/images.

The Yellowknife dataset was chosen to apply the regression model, which will be seen in subsection 1.4.1. We use the Ljung-Box's test (Trapletti, 2016) to choose the block size N such that the minimum sub-sample of these blocks are independent. For the Yellowknife data, the test does not reject the null hypothesis of independence for $N >= 20$. For this reason, and to capture the minimum of each year's season, we consider $N = 90$.

Table 1.3: Descriptive measures for datas

Data	Mean	Min C°	1st Qua	Median	3st Qua	Max C°
Svalbard	-4.39	-21.80	-9.40	-4.80	1.60	9.70
Dawson City	0.54	-44.90	-15.10	3.40	17.70	29.10
Yellowknife	-27.42	-48.90	-41.70	-34.40	-9.70	5.20
Delhi	21.71	11.00	16.44	19.88	27.71	34.50

In table 1.3, the descriptive measures for data is detailed. As expected, as the dataset corresponds to minimum temperature, the city of Yellowknife has the lowest minimum temperature and mean of all datasets. Delhi, being the only city that is in south hemisphere, has the highest maximum temperature and mean of all.
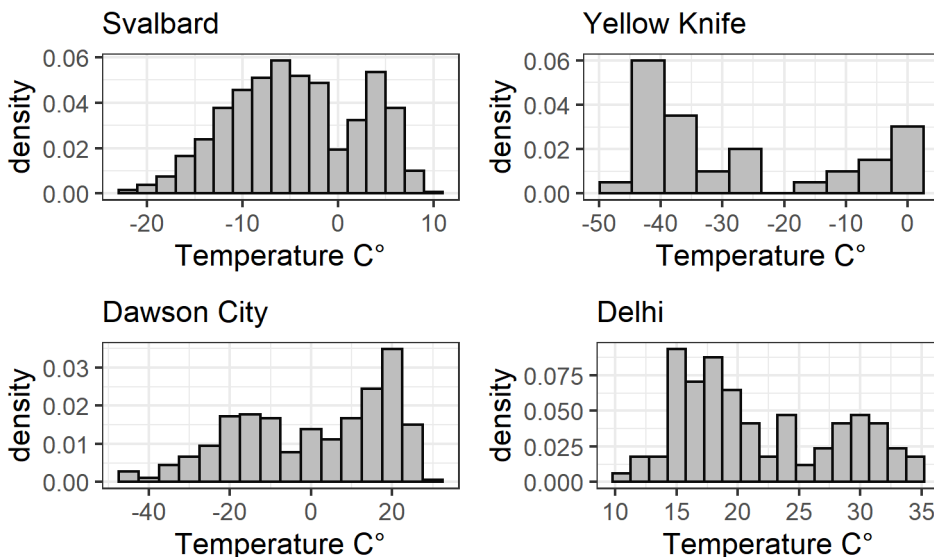
Figure 1.13: Original temperature data

In Figure 1.13 are the histograms of the four data sets corresponding to the original data.

When considering the population of the data as a random variable X, whose density presents a bimodal behavior with positive and negative values, we transform these data into non-negative using the function $Y = \exp(X/100)$ for Dawson City, Yellowknife and Delhi and $Y = \exp(X/10)$ for Svalbard. Following that, we fit the transformed data in NNIBW model, $F_{NNIBW}(.; \beta, \delta, \mu, \lambda)$, and in the BWeibull model $F_{BWeibull}(.; \alpha, \beta, \delta)$, (Vila and Niyazi Çankaya, 2021).

To fit the Y data, the maximum likelihood procedure was used to estimate the parameters. In R Project for Statistical Computing, version 4.0.5 we estimate the parameters by optimizing the log-likelihood function of each model through the *optim* function. As the optimization procedure requires the input of initial values, a range of values for each parameter were created based on the values seen in Figures 1.6 and 1.7. Then this range was used to define a grid of length 1000 of different initial values for optimization.

The estimates result of the parameters for the four data sets and the results of the goodness-of-fit test based on the Akaike Information Criterion (AIC) are shown in Table 1.4. This table shows that the NNIBW model is the most suitable, judging the AICs. Figure 1.14 also shows that the NNIBW model fits these bimodal data better than the BWeibull model.

Table 1.4: Estimates and AIC for each model

Data	BWeibull			NNIBW			
	$\hat{\alpha}$	$\hat{\beta}$	$\hat{\delta}$	$\hat{\beta}$	$\hat{\lambda}$	$\hat{\delta}$	$\hat{\mu}$
Svalbard	1.858352	0.890644	1.105322	2.0982	1.0225	0.5414	-1.1030
AIC		2082.366				1893.531	
Yellowknife	4.7991	0.760	-0.00023	84.26952	0.66067	1.6551	-0.6626
AIC		-295.8803				-510.1072	
Dawson City	7.010053	1.106196	0.780132	19.5989	1.1025	0.6753	-1.0883
AIC		-218.1242				-319.274	
Delhi	14.51825	1.267309	3.61872	205.6770	1.6910	1.0227	-1.6929
AIC		-227.9446				-281.8058	

Comparing the models results shown in table 1.4, the NNIBW model gives a better value

for the AIC than the BWeibull model.The $\hat{\mu}$ being negative for the four datasets were expected, since it gives the bimodality shown on the Figure 1.14, but $\hat{\beta}$ appears to be overestimated. The BWeibull model was unable to show the bimodality on the datasets, one of the reasons can be that, on the paper, this function has shown bimodality only on larger scale data and the model probably has difficulties to be fitted to a smaller range of X (Vila and Niyazi Çankaya, 2021).
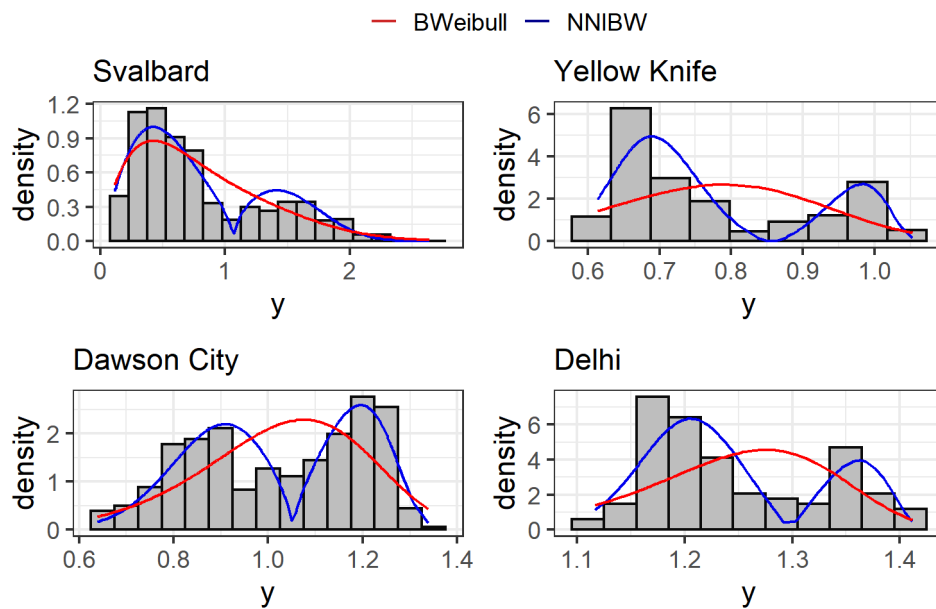

Figure 1.14: NNIBW and BWeibull densities fitted to the transformed data.

The good fit of the data by the NNIBW model is also shown in Figures 1.15-1.18, since the theoretical functions of the CDF and Quantile of the NNIBW model are close to their respective empirical functions.
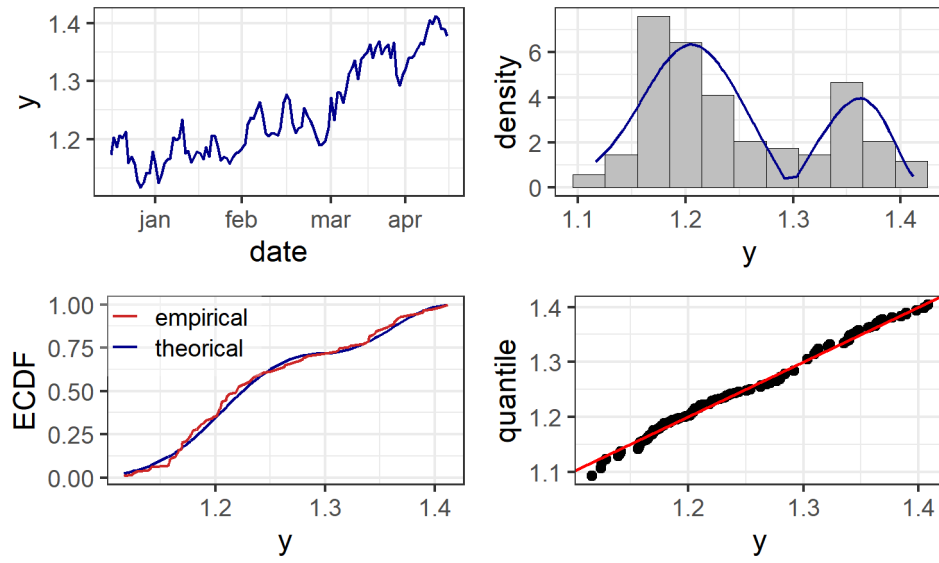
Figure 1.15: Delhi: Historical series, fitted density, CDF, and quantile function.
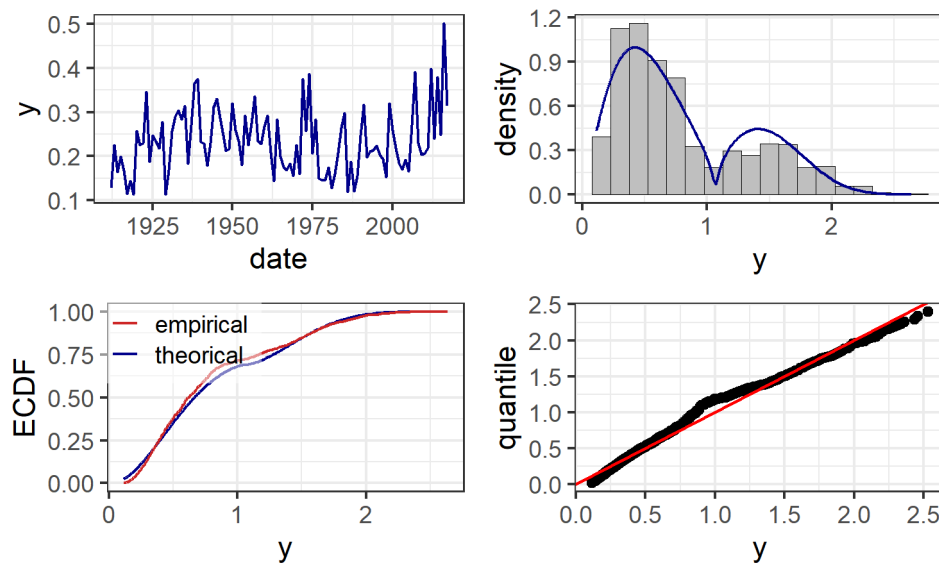
Figure 1.16: Svalbard: Historical series, fitted density, CDF, and quantile function.
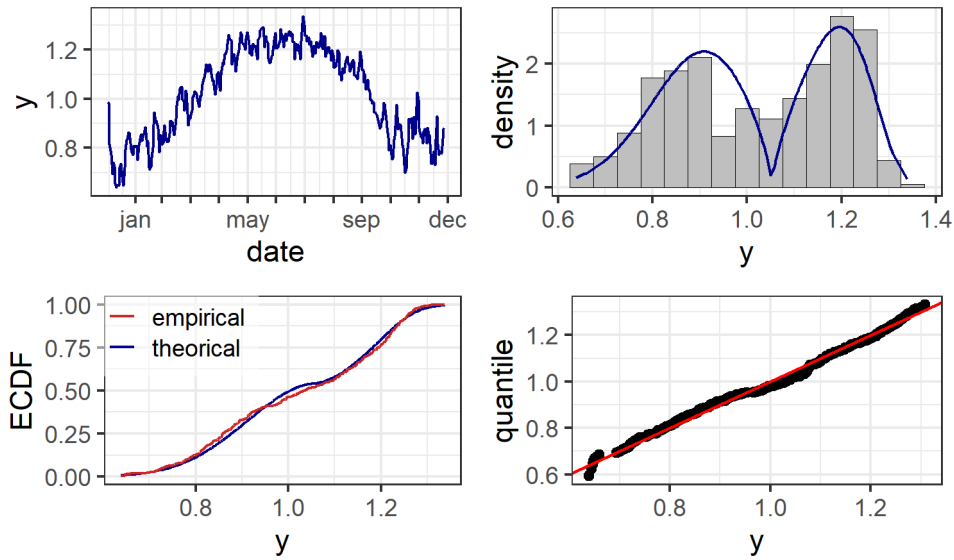
Figure 1.17: Dawson City: Historical series, fitted density, CDF, and quantile function.
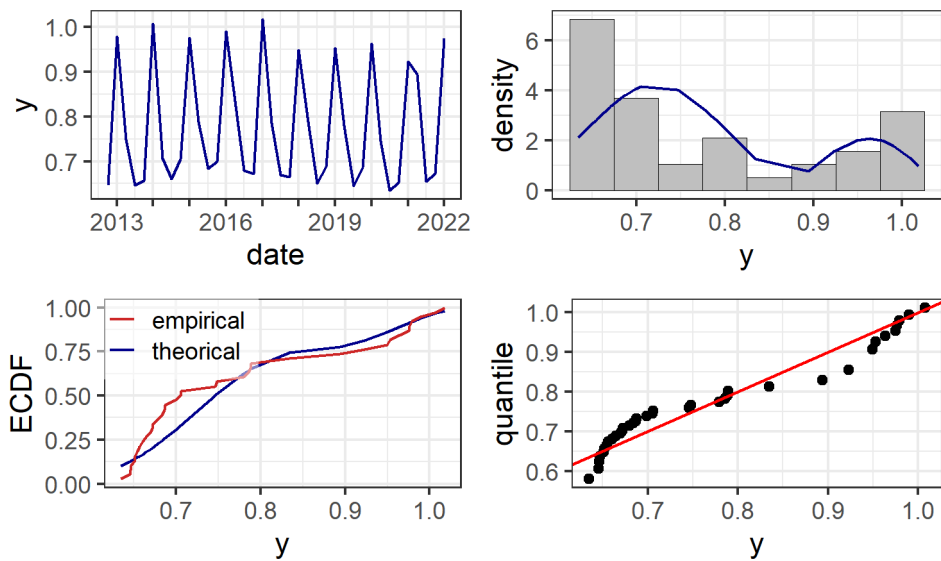
Figure 1.18: Yellowknife: Historical series, fitted density, CDF, and quantile function.

The temperature is an event that can be associated with a return time. This statistical function is very useful for risk analysis in climatology, generally to minimize the harmful effects of temperature. From the equations 1.2.18 and 1.2.19, it can be seen that for an NNIBW population the return level has a closed formula. Based on the quantile function 1.2.19, here the

return level and return time of Y were calculated, and then, by the transformation $100 \ln(Y)$, the return level and return time of the original data X were obtained. Figures 1.19 to 1.22 illustrate the return level and return time for the four data sets. In the left panels is the return time of the transformed data and in the right panels is the return time of the original data.
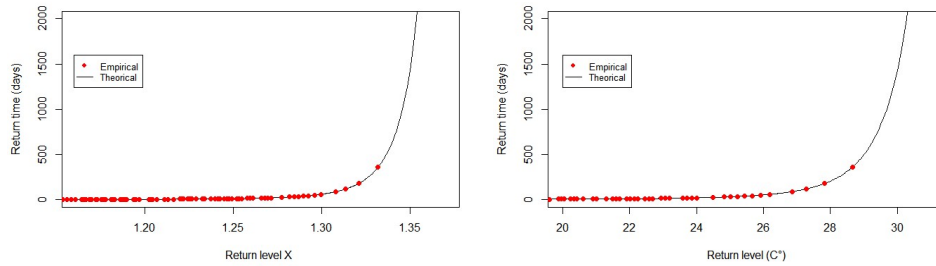
Figure 1.19: Return time of Dawson City: original data (right panel) and transformed data (left panel).
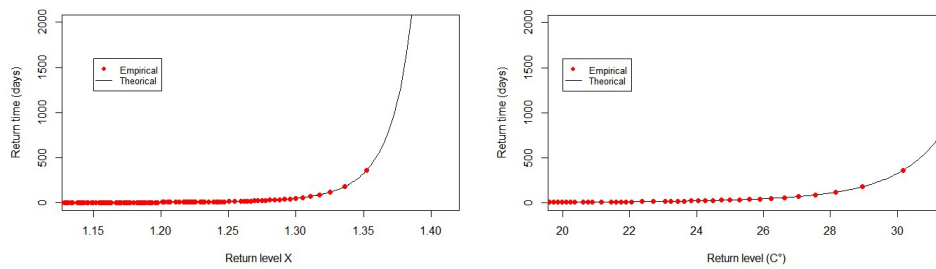
Figure 1.20: Return time of YellowKnife: original data (right panel) and transformed data (left panel).
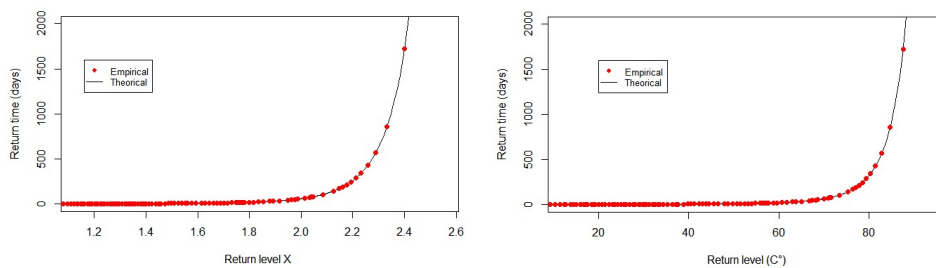
Figure 1.21: Return time of Svalbard: original data (right panel) and transformed data (left panel).
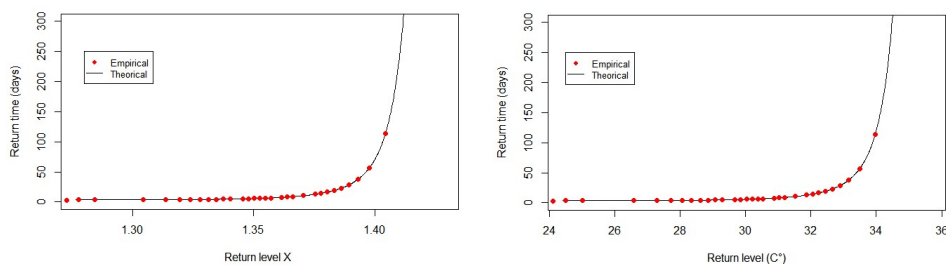
Figure 1.22: Return time of Delhi: original data (right panel) and transformed data (left panel).

The real applicability of our model in risk analysis is through the return time. To make this clearer, in Table 1.5, we show seven particular values of the return time and their corresponding return level for Dawson City, Yellowknife, Svalbard, and Delhi.

Table 1.5: Some return time and return level values.

	p	Return time	Return Level °C
Dawson City	0.375	1.6	-6.73
	0.5	2	0.35
	0.9	10	21.69
	0.95	20	23.85
	0.99	100	27.01
	0.999	1000	29.68
Yellowknife	0.375	1.6	-36.40
	0.5	2	-32.61
	0.9	10	-1.23
	0.95	20	0.77
	0.99	100	3.28
	0.999	1000	5.16
Svalbard	0.375	1.6	-6.47
	0.5	2	-4.08
	0.9	10	4.91
	0.95	20	5.88
	0.99	100	7.30
	0.999	1000	8.53
Delhi	0.375	1.6	18.62
	0.5	2	20.29
	0.9	10	31.45
	0.95	20	32.50
	0.99	100	33.88
	0.999	1000	34.97

In table 1.5, the interpretation is different for each city. As instance for Dawson City, the return time is given as days for the maximum temperature, on the mean, it takes 100 days to overcome 27.01 °C. For Svalbard, as the data is the monthly average, 100 months are expected to experience at least once the mean temperature of 3.28 °C . For Yellowknife, as the data are the minimum value of 90 days, the return time must be interpreted as sets of this length, so, 9000 days are expected to overcome a minimum temperature of 3.28 ℃.

1.4.1   Regression model

A NNIBW regression model can be obtained by incorporating the regressor variables into the NNIBW distribution through the parameter λ. Thus, considering the log-link function, the NNIBW regression model is given by expression (1.2.22) with

$$\lambda = \exp\{Z'\gamma\}, \tag{1.4.1}$$

where $Z = (1, Z_1, \ldots, Z_k)$ is the vector of k explanatory variables with their respective regression coefficients given by $\gamma = (\gamma_0, \gamma_1, \ldots, \gamma_k)$.

A regression model allows explaining the relationship between the explanatory variables in the event of interest. To investigate the influence of seasons on the Yellowknife temperature, here we consider a NNIBW regression model in the λ parameter. Since the data corresponds to the period of quarters of year, each observation can be classified according to four seasons (Summer, Winter, Autumn or Spring). In this example, the four seasons were considered as an explanatory variable associated to temperature. Since it has four categorical levels, three dummies variables were defined: Z_1, Z_2 and Z_3, where $Z_1 = 1$ if it is Winter and $Z_1 = 0$ otherwise; $Z_2 = 1$ if it is Autumn and $Z_2 = 0$ otherwise; $Z_3 = 1$ if it is Spring and $Z_3 = 0$ otherwise. Here, the Summer was considered as the reference category (represented as $Z_1 =$

$Z_2 = Z_3 = 0$). Thus the NNIBW regression model is given by expression (1.21) with

$$\lambda = \exp\{\gamma_0 + \gamma_1 Z_1 + \gamma_2 Z_2 + \gamma_3 Z_3\}. \tag{1.4.2}$$

In (1.4.2) γ_0 is the regression coefficient associated to Summer and γ_1, γ_2 and γ_3, are the regression coefficients associated to Winter, Autumn and Spring, respectively. The estimates of the parameters of the NNIBW regression model were calculated by optimizing the likelihood function (2.5) using the optimal function of the R program. Table 1.6 presents the results of parameter estimates from the NNIBW regression model for the Yellowknife City dataset.

Table 1.6: Parameters estimates for the regression model

parameter	estimate
γ_0	0.317
γ_1	-0.088
γ_2	-0.013
γ_3	-0.060
β	49.135
δ	0.932
μ	-0.691

These results is being interpreted as follows: The greater the value of γ the greater the value of the temperature associated with the corresponding season. Thus, our results are coherent with reality, since the coefficient γ_1 associated with Winter is the lowest value and the coefficient corresponding to Summer, γ_0, is the highest value. The Autumn and Spring coefficients, γ_2 and γ_3, respectively, are intermediate. The illustration of our regression model is shown in Figure 1.23. It can be seen that the data for all seasons were well-adjusted by the NNIBW model and Winter and Summer seasons were well-defined by an unimodal density, while the Autumn and Spring seasons are diversified and explained by bimodal densities.
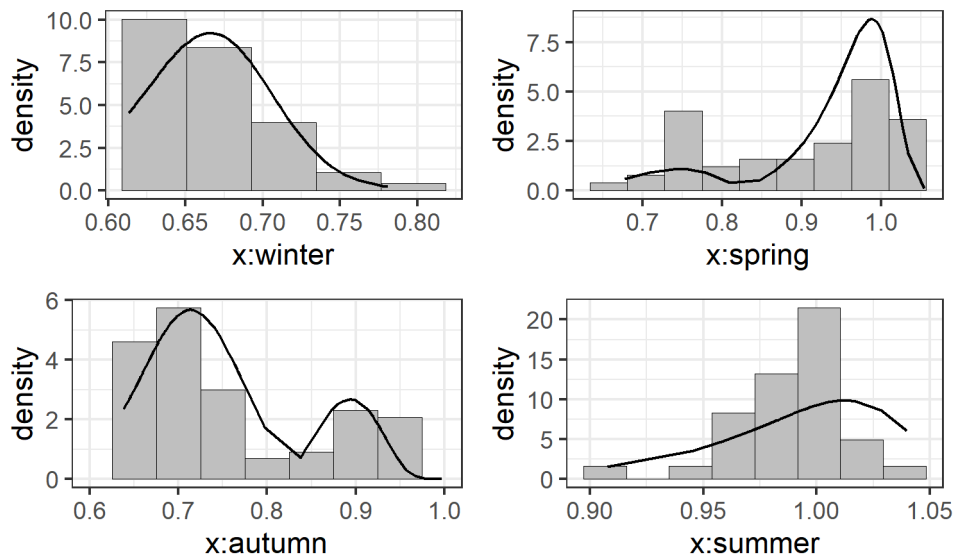
Figure 1.23: Fitted regression model for Yellowknife data

1.4.2 Concluding Remarks

In this paper, a new generalization of the Weibull distribution were proposed with two resulted distributions: the Invertible Bimodal Weibull and the Non-negative invertible Bimodal Weibull. The NNIBW has shown different formats and flexibility on PDF, CDF and HRF functions. The estimation of the parameters and the simulation of the distribution were uncomplicated to accomplish, due to the model's closed form. The application of the model in the chosen datasets were satisfied, which shows that this model can be applied to studies about weather and temperature. Overall, the results were satisfactory, and the regression model allowed explaining the relationship between the variables. As future work we can point out the study of the NNIBW model in the context of dependent data.

Appendix A
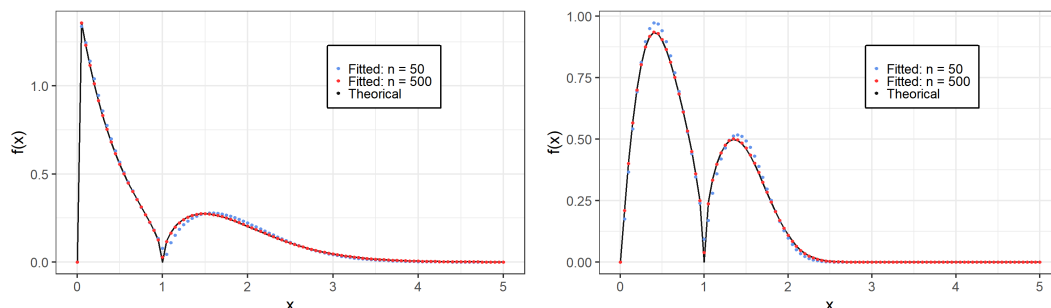
Figure 24: Theoretical density versus adjusted density: $f_{NNWBI}(x; \theta_i)$ $i = 1$ (left) and 2 (right).
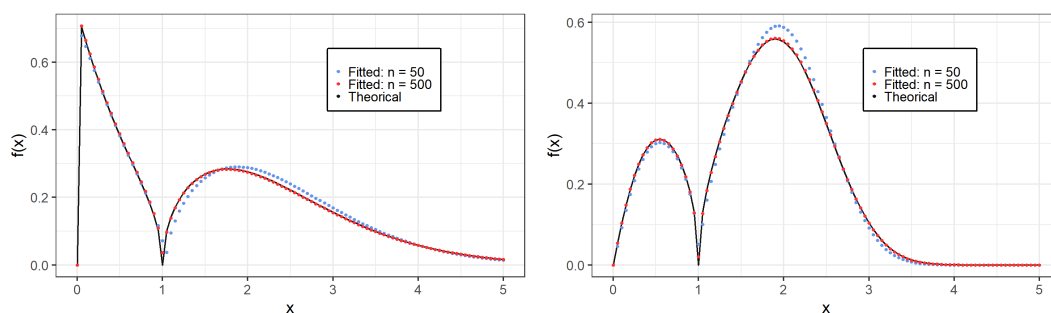
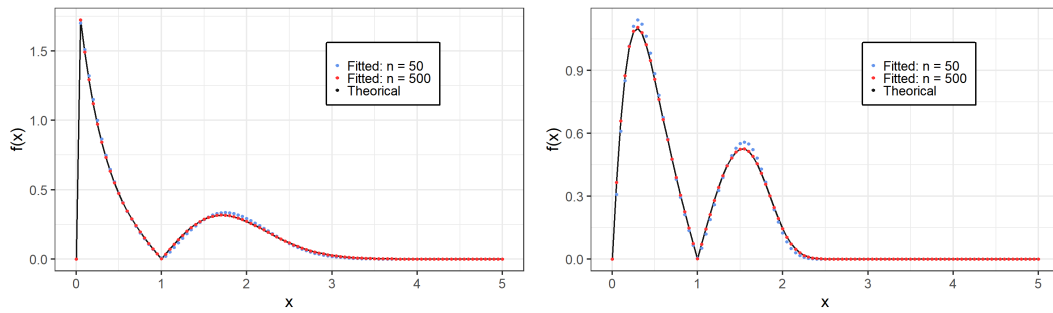**Figure 25:** Theoretical density versus adjusted density: $f_{NNWBI}(x; \theta_i)$ $i = 3$ (left) and 4 (right).

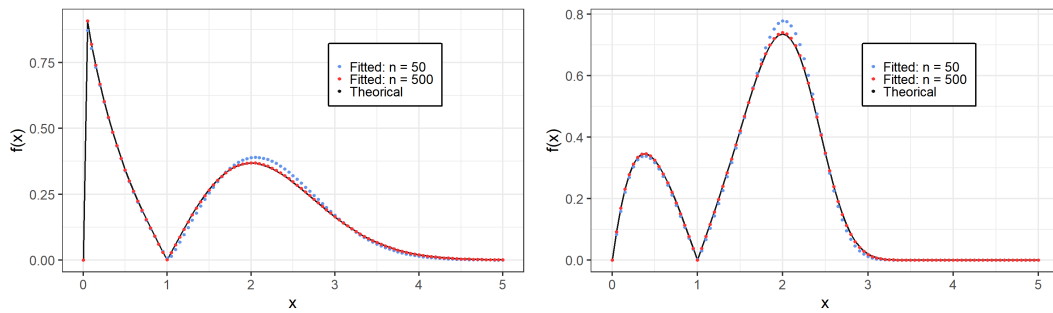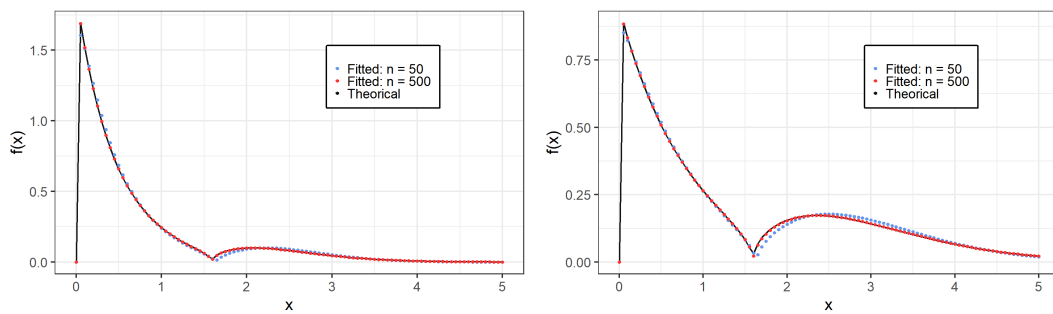**Figure 26:** Theoretical density versus adjusted density: $f_{NNWBI}(x; \theta_i)$ $i = 5$ (left) and 6 (right).

Figure 27: Theoretical density versus adjusted density: $f_{NNWBI}(x; \theta_i)$ $i = 7$ (left) and 8 (right).

Figure 28: Theoretical density versus adjusted density: $f_{NNWBI}(x; \theta_i)$ $i = 9$ (left) and 10 (right).
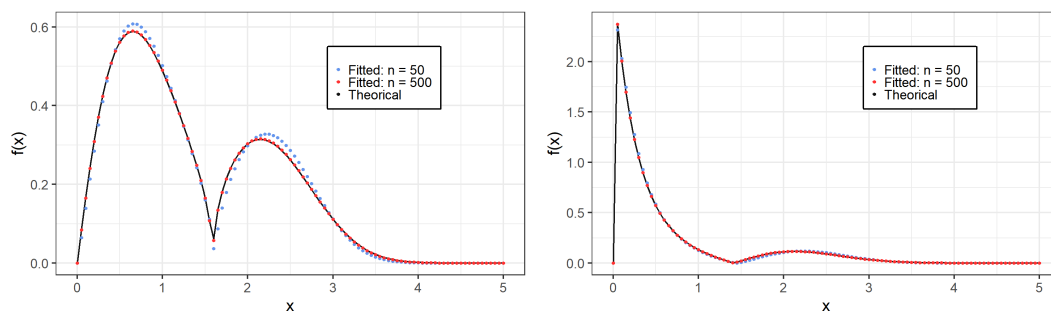
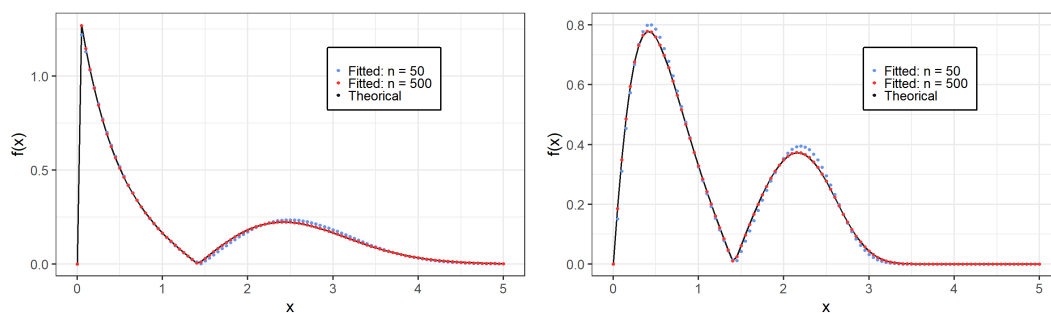**Figure 29:** Theoretical density versus adjusted density: $f_{NNWBI}(x; \theta_i)$ $i = 11$ (left) and 12 (right).

Figure 30: Theoretical density versus adjusted density: $f_{NNWBI}(x; \theta_i)$ $i = 13$ (left) and 14 (right).

References

Climate Weather (2022). `https://climate.weather.gc.ca`. Access on: 12/02/2022.

Daily Climate time series data (2022). `https://www.kaggle.com/datasets/sumanthvrao/daily-climate-time-series-data`. Access on: 12/02/2022.

Domma, Filippo, Popović, Božidar V, and Nadarajah, Saralees (2015). "An extension of Azzaliniâs method". In: *Journal of Computational and Applied Mathematics* 278, pp. 37–47.

Kumar, DEVENDRA and Dey, SANKU (2017). "Power generalized Weibull distribution based on order statistics". In: *Journal of Statistical Research* 51.1, pp. 61–78.

Lee, Carl, Famoye, Felix, and Olumolade, Olugbenga (2007). "Beta-Weibull distribution: some properties and applications to censored data". In: *Journal of modern applied statistical methods* 6.1, p. 17.

McLachlan, G and Peel, D (2000). *Finite mixture models.,(john wiley & sons: New york.)*

Mudholkar, Govind S and Srivastava, Deo Kumar (1993). "Exponentiated Weibull family for analyzing bathtub failure-rate data". In: *IEEE transactions on reliability* 42.2, pp. 299–302.

Pena-Ramirez, Fernando A et al. (2018). "The exponentiated power generalized Weibull: Properties and applications". In: *Anais da Academia Brasileira de Ciências* 90, pp. 2553–2577.

Seber, George AF and Lee, Alan J (2003). "Wiley series in probability and statistics". In: *Linear Regression Analysis*, pp. 36–44.

Svalbard Climate, 1910-2017 (2022). `https://www.kaggle.com/datasets/dbialer/svalbard-climate-19102017`. Access on: 12/02/2022.

Trapletti, A (2016). *R: Box-Pierce and Ljung-Box Tests. stat. ethz. ch*. Tech. rep. Retrieved 2016-06-05. URL https://stat. ethz. ch/R-manual/R-devel/library â¦.

Vila, Roberto and Niyazi Çankaya, Mehmet (2021). "A bimodal Weibull distribution: properties and inference". In: *Journal of Applied Statistics*, pp. 1–19.

Zaindin, Mazen and Sarhan, Ammar M (2009). "Parameters estimation of the modified Weibull distribution". In: *Applied Mathematical Sciences* 3.11, pp. 541–550.